

Beam self-trapping in a BCT crystal

V. Matusevich*, A. Kiessling*, R. Kowarschik*, A.E. Zagorskiy**, V.V. Shepelevich**

*Friedrich-Schiller-University Jena, Institute of Applied Optics

**Mozyr State Pedagogical University, Laboratory of Coherent Optics and Holography-

mailto: Vladislav.Matusevich@uni-jena.de

We present some aspects of wave self-focusing and self-defocusing in a photorefractive $Ba_{0.77}Ca_{0.23}TiO_3$ (BCT) crystal without external electric field and without background illumination. The effects depend on the cross-section of the input beam. We show that by decreasing of the diameter of the input beam from 730 μm the fanning effect disappears at 150 μm . A symmetrical self-focusing is observed for input diameters from 150 μm down to 40 μm and a symmetrical self-defocusing for input diameters from 40 μm down to 20 μm . The 1D self-trapping is detected at 65 μm in BCT. Light intensity and wavelength are correspondingly 3 mW and 633 nm. The experimental results are supplemented with numerical calculations based on both photovoltaic model and model of screening soliton.

1 Introduction

In this paper we present observations of self-focusing and self-defocusing in a BCT crystal in dependence on the beam cross-section and explain them, whereas neither an external electric field nor a background illumination is applied.

2 Experiment

A He-Ne laser is the source of the linearly extra-ordinarily polarized monochromatic (633 nm) wave with a power $P = 3$ mW. The lens L1 focuses the wave so that the beam waist is located on the front surface of the BCT crystal. The lens L2 (microscope-objective with magnification 10 and NA 0.25) and the CCD-camera with the pixel size of 6.8 μm take the pictures of the input beam (without the crystal) and of the output beam (on the rear surface of the crystal) (Fig. 1).

We vary the diameter¹ of the input beam from 730 μm down to 17 μm by using lenses (L1) with different focal distances and measure the profile of the output beam. For each experiment the profile of the input beam is measured to control that the minimal beam waist is located at the entrance surface of the crystal. Neither an electric field nor a background illumination is applied.

¹ We define the diameter from the intensity distribution

$I = I_0 e^{-\frac{x^2+y^2}{\omega_0^2}}$ as $2 \omega_0$, whereas the field

distribution is given by $u = \sqrt{I_0} e^{-\frac{x^2+y^2}{2\omega_0^2}}$.

By decreasing of the diameter of the input beam from 730 μm down to 150 μm the fanning decreases steadily. At 150 μm the fanning disappears completely and no more fanning can be observed for smaller diameters. Exact at this diameter the first self-focusing effect in x-dimension becomes apparent (Fig. 2).

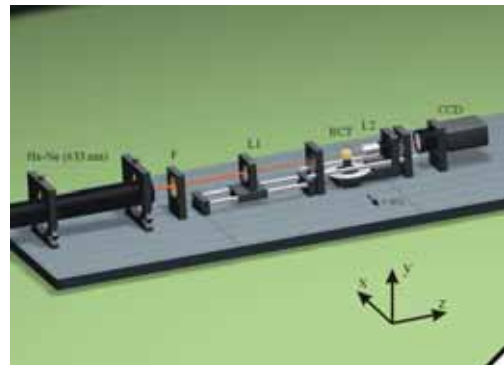


Fig. 1 Experimental setup. F is filter, L1 is converging lens, and L2 is microscope-objective. The path between the lens L1 and the crystal BCT corresponds to the focal distance of the lens L1, so that the beam is focused on the front surface of the crystal..

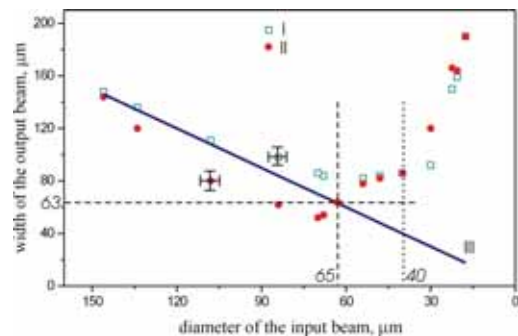


Fig. 2 Cross-section of the output beam in dependence of the diameter of the input beam. I y-size of the output beam (perpendicular to the c-axis) (unperturbed Gaussian beam), II x-size of the output beam (parallel to the c-axis), III straight line corresponds to equal input and output diameters.

3 Theory

The equation of beam propagation in a photorefractive medium in a paraxial approximation has the form

$$i \frac{\partial E}{\partial z} + \frac{1}{2k_0 n_0} \left(\frac{\partial^2 E}{\partial x^2} + \frac{\partial^2 E}{\partial y^2} \right) - \frac{k_0 n_0^3}{2} r_{33} E_{sc} E = 0, \quad (1)$$

where $k_0 = 2\pi/\lambda$, λ is the wavelength in vacuum, n_0 is the refractive index of the crystal, E_{sc} is the space-charge field, E is the strength of the electric field of the light wave. For simplification we write the strength of the electric field of the light wave as

$$E(x, y) = \sqrt{I_{\max}} u(x, y), \quad (2)$$

where I_{\max} is the maximal value of the intensity of the light beam, $u(x, y)$ is a non-dimensional function, and we introduce a new constant

$$N = \frac{I_{\max}}{I_d} \quad (3)$$

with the dark intensity I_d of the crystal.

Photovoltaic model

A light beam initiates in a photorefractive crystal a space-charge field, which is given by the relationship

$$E_{sc}(x, y) = E_p \frac{\sqrt{N} |u(x, y)|}{\sqrt{1 + N |u(x, y)|^2}} \quad (4)$$

in case of the local approximation, where $E_p = k_p \gamma_R N_A / (e\mu)$ is the photovoltaic field, k_p is the photovoltaic constant, γ_R is the recombination rate, N_A is the density of acceptors, e is the elementary charge, μ is the charge mobility.

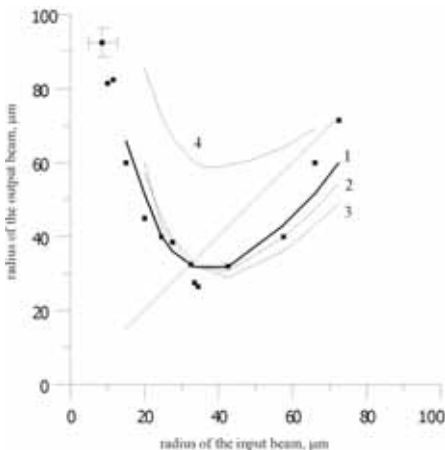


Fig. 3 Dependence of the output beam radius on the radius of the input beam for the photovoltaic model. The experimental results are depicted by points. The graphs correspond: graph 1 – $E_0=450$ V/cm $N=0.5$; graph 2 – $E_0=440$ V/cm $N=1$; graph 3 – $E_0=510$ V/cm $N=2$; graph 4 – divergence in a linear medium. The straight line corresponds to equal widths of input and output beams.

Model of screening solitons

Let us suggest now that there is an internal coercitive electric field E_0 parallel to the c-axis of the crystal. Then the relationships of yield

$$E_{sc}(x, y) = E_0 \frac{1}{\sqrt{1 + N |u(x, y)|^2}}, \quad (5)$$

where E_0 corresponds to E_{eff} .

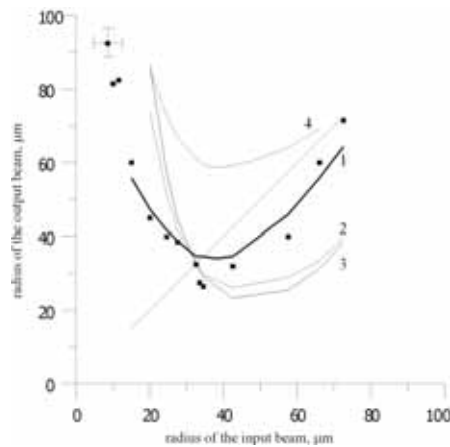


Fig. 4 Dependence of the output beam radius on the radius of the input beam for the model of screening solitons. The experimental results are depicted by points. The graphs correspond: graph 1 – $E_0=400$ V/cm $N=0.1$; graph 2 – $E_0=800$ V/cm $N=1.5$; graph 3 – $E_0=1600$ V/cm $N=10$; graph 4 – divergence in a linear medium. The straight line correspond to the equal width of input and output beams.

The theoretical results prove that photovoltaic effects do not appear most likely, while one can observe a good coincidence of the model of screening solitons with experimental results, whereas the internal coercitive electric field corresponds to the external applied electric field.